IEEE Access
Multidisciplinary | Rapid Review | Open Access Journal

Received August 14, 2019, accepted August 30, 2019, date of publication September 3, 2019,
date of current version September 19, 2019.

Digital Object Identifier 10.1109/ACCESS.2019.2939270

A Low Correlation and Mutual Coupling MIMO Antenna

YING LIU[1], (Senior Member, IEEE), XU YANG[1], YONGTAO JIA[1], (Member, IEEE), AND Y. JAY GUO[2], (Fellow, IEEE)

[1]Science and Technology on Antenna and Microwave Laboratory, Xidian University, Xi'an 710071, China
[2]Global Big Data Technologies Center, University of Technology Sydney, Sydney, NSW 2007, Australia

Corresponding author: Ying Liu (liuying@mail.xidian.edu.cn)

This work was supported by the National Natural Science Foundation of China under Grant 61871309.

ABSTRACT A new two-element multiple-input multiple-output (MIMO) antenna with low correlation and high port isolation is presented. First, two hybrid electromagnetic band gap (EBG) structures with the ability to support and stop surface wave propagation, respectively, are utilized simultaneously for achieving an extremely low envelope correlation coefficient (ECC). Then, based on studying of the ground current of the MIMO antenna with EBG structure, a new defected ground structure (DGS) is used to reduce the mutual coupling by controlling the polarization of the coupling field. The two antenna elements have an edge to edge spacing of 0.13λ where λ is the free space wavelength at the resonant frequency. Finally, the rectangular slots are introduced to the patch to improve the cross polarization. Experimental results show that the ECC of the MIMO antenna is lower than 0.002. Furthermore, the maximum mutual coupling (MC) reduction of 22dB can be achieved within the working bandwidth. All of above make the MIMO antenna a potential candidate for mobile terminal-based MIMO antenna systems.

INDEX TERMS Multiple-input multiple-output (MIMO) antenna, envelope correlation coefficient (ECC), defected ground structure (DGS), electromagnetic band gap (EBG).

I. INTRODUCTION

The MIMO antenna is widely regarded as an effective technology to improve channel capacity and increase data throughput in wireless communications systems, thus making it key to the fifth generation (5G) communications networks. Besides the millimeter wave bands, the sub-6GHz frequency band, for example 4.9GHz frequency band in China, is also one of important 5G spectrum resources. Hence, MIMO antennas working in the 4.9GHz band are becoming a hot research topic.

The correlation coefficient (CC) or envelope correlation coefficient (ECC) of a MIMO antenna is commonly used to measure the quality of the channel correlation. It can be calculated by using three dimensional (3D) radiation patterns of a MIMO antenna system. Additionally, for antennas which are lossless in an isotropic environment, the ECC can also be calculated by S-parameters. Therefore, to improve ECC and channel capacity, several methods have been investigated. In [1], a MIMO antenna with an orthogonally reconfigurable radiation pattern was investigated to achieve lower ECC and high isolation. A similar method can also be found in [2], [3]. For the MIMO antenna presented in [2], polarization diversity and complementary split-ring resonators (CSRR) are utilized to reduce ECC. Another way to control ECC is by using radiation pattern diversity. The Fabry-perot (FP) antenna with phase gradient frequency selective surface (FSS) was studied in [4]. The antenna could realize 95% correlation coefficient value reduction by tilting the beam direction. However, the large lateral size and high profile limited its application. Moreover, some MIMO antennas can also achieve a low correlation by using port isolation enhancement techniques, such as metamaterials [5], coupled resonator decoupling networks (CRDN) [6], tree-like isolators [7] and parasitic branches [8].

When antenna elements are placed in a limited space, mutual coupling between the adjacent ports is another significant figure of merit for a MIMO antenna. In [9], [10], EBG structures were utilized to improve port isolation by virtue of band gap characteristic. However, to obtain low mutual coupling, these EBG structures often need a larger space to form the periodic arrangement, which is not beneficial to the miniaturization design of MIMO antennas for mobile terminals.

The associate editor coordinating the review of this manuscript and approving it for publication was Lu Guo.

In [9], a novel mushroom-like EBG structure was utilized to suppress the mutual coupling between two patch antennas and an isolation enhancement of 26dB was achieved. Unfortunately, the center to center spacing of about 0.6λ would lead to a large lateral size. Thus, to reduce the mutual coupling between two closely spaced elements, the decoupling surface superstrates were placed above the compact antenna array in [11]–[14]. An array antenna decoupling surface (ADS) [12] was designed to cancel the coupling fields generated by the antenna array, which resulted in high port isolation. The antenna elements were also placed very closely. Reference [14] proposed a near-field resonator surface for reducing mutual coupling. This technique could improve the isolation by 20dB and the edge separation between the two antennas was only 0.016λ. However, although these designs can achieve an extremely close antenna separation and low mutual coupling, antenna arrays covered with superstrates would increase the antenna profile and cost. Defected ground structures proposed in [15]–[18], as an alternative decoupling solution, can be easily fabricated and do not need any extra structures. In [15], a simple rectangular resonant slot etched on the groundplane of the two antenna system was used to improve the isolation effectively and the center to center distance of the two antennas was 0.33λ. As for [16], by using the third iterative structure of the fractal DGS, a significant mutual coupling reduction between the two coplanar spaced antennas was achieved. Compared with the reference antenna, the fractal DGS caused a resonant frequency shift. The ECC calculated by S-parameters was not accurate, which could be known from [19].

In this paper, we present a new two-element MIMO antenna with low correlation and high port isolation. First, two hybrid EBG structures are employed in a two element MIMO patch antenna for achieving an extremely low ECC. Different from most EBGs which are mainly used to suppress the coupling surface wave in a MIMO antenna system [5], [9], [10], the two different EBG structures are adopted to realize radiation pattern diversity. One of them is the traditional EBG structure placed in the middle of the two antennas and designed to stop surface wave propagation. The other EBG is placed on the two sides of the antenna elements and works in the zone of surface wave propagation to guide surface wave sideway. Thus, good radiation pattern diversity caused by the tilted beams can be realized within the bandwidth. To further enhance the decoupling, a new DGS is introduced. Different from the traditional ones [15]–[18] that aim to stop coupling current from one port to another port, the new DGS aims to change the polarization of the coupling field. In addition, rectangular slots are employed in the patch to improve the cross polarization of the antenna effectively. The combination of these techniques results in low correlation and high port isolation of the proposed MIMO antenna. The measured results show that the MIMO antenna has an edge to edge distance of 0.13λ between the two patches and a low ECC value that is lower than 0.002. The maximum isolation enhancement of 22dB can be obtained within the working frequency band. Also, the MIMO antenna has a low profile of 0.02λ. A prototype is manufactured and measured. The simulated and measured results agree with each other well.

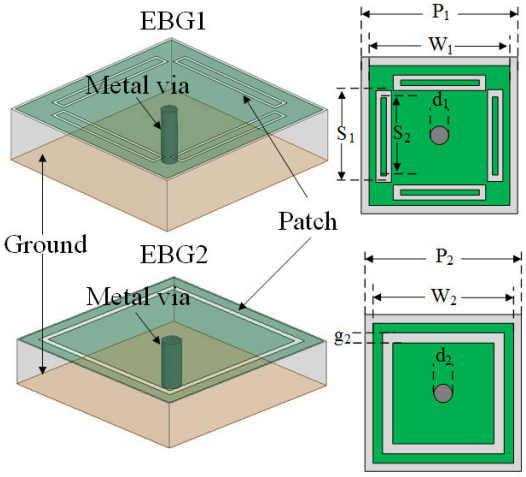

FIGURE 1. Configuration of the two EBG structures.

The rest of this paper is organized as follows. Section II analyzes the two EBG structures and the DGS which are employed in the MIMO antenna. The measured and simulated results are shown and discussed in Section III. Section IV gives a brief conclusion.

II. ANTENNA DESIGN AND ANALYSIS

A. ELECTROMAGNETIC BAND GAP DESIGN

The reference MIMO antenna consists of two patch antennas working in the 4.9GHz frequency band. The two patches are printed on an FR4 substrate whose dielectric constant is 4.4 and loss tangent is 0.02. The center to center separation is 0.36λ (edge to edge distance of 0.13λ). These two patch antennas share a common ground plane. The height of the substrate is 1.5mm. The antenna structure is simulated by the high frequency structure simulator (HFSS ver. 15).

EBG structure is derived from the photonic band gap (PBG). It can be constituted by 2D/3D periodic metals or a mixture of metal and dielectric components. Usually, there are two features of EBG including in phase reflection coefficient and surface wave suppression, however, according to [20], the EBG structure can also work as the high impedance surface (HIS) to support surface wave propagation. Hence, beam steering can be realized with hybrid EBG structures via controlling the diffusion path of surface waves. In the reported work, two proposed mushroom-like EBG structures are shown in Fig.1. They are designated as EBG1 and EBG2, respectively. EBG1 is composed of a metal via and a square patch on which four rectangular ring slots are etched for miniaturization. By adjusting the slots, EBG1 can prevent surface wave propagation in the 4.9GHz band. The patch of EBG2 is a combination of a square ring and a square patch to reduce the surface current path. Therefore, the

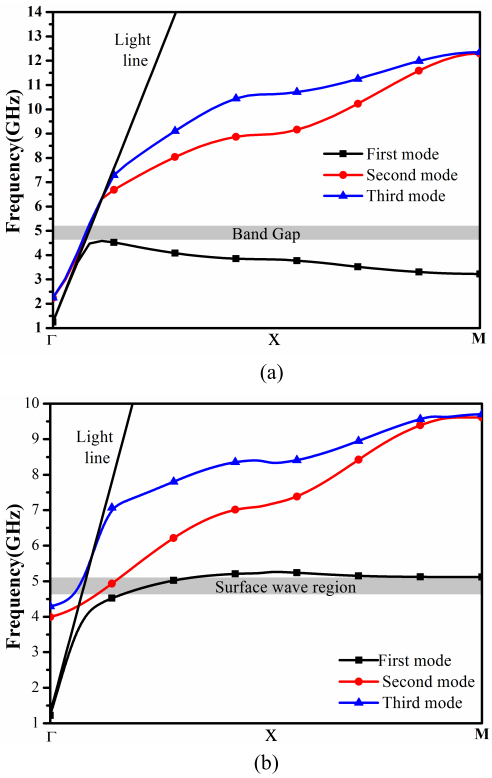

FIGURE 2. Dispersion diagrams of the two EBG structures. (a) EBG1, (b) EBG2.

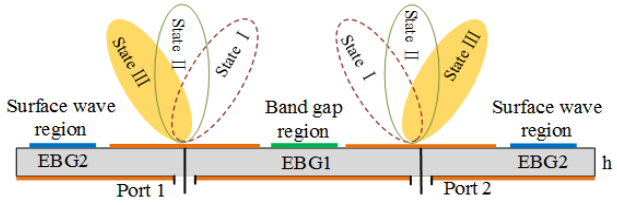

FIGURE 3. Tilted beam schematic diagram of the MIMO antenna with EBG structures.

stop band can be moved to the higher frequencies, which means that EBG2 can support surface wave propagation in the desired band. The dispersion diagrams of the two EBG structures are plotted in Fig. 2. It can be observed that the two EBGs can work in the band gap region and TM surface wave propagation region respectively in the 4.9GHz band.

B. HYBRID EBG STRUCTURE APPLICATION

$$|\rho_{12}|^2\,(CC) = \rho_e\,(ECC) = \frac{\left|\int\int_{4\pi}\left[E_1\,(\theta,\phi) * E_2\,(\theta,\phi)\right]d\Omega\right|^2}{\int\int_{4\pi}|E_1\,(\theta,\phi)|^2\,d\Omega\int\int_{4\pi}|E_2\,(\theta,\phi)|^2\,d\Omega} \tag{1}$$

Generally, in an isotropic wireless communication environment, especially for the printed MIMO antenna which is

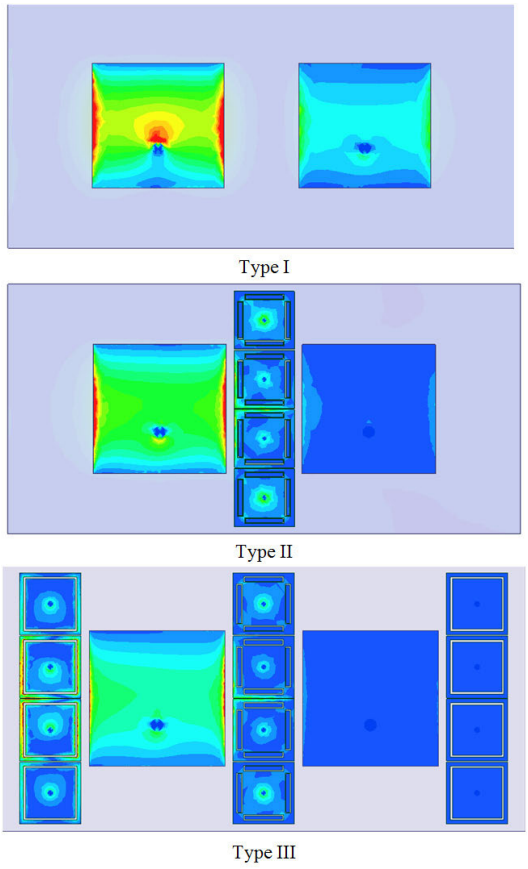

FIGURE 4. Surface currents distribution of the three MIMO antennas at 4.95GHz.

lossy, the envelope correlation coefficient of a two element-based MIMO antenna should be calculated by the formula (1) [21] where indicates a complex 3D radiation pattern of the antenna element i. To achieve a better channel isolation or low ECC, an efficient method is needed to isolate the two antenna beams spatially.

When two antennas are placed very closely, the mutual coupling between the two antennas can result in lots of problems. Besides the port isolation being severely influenced, the radiation beam will also deteriorate because of the strong induced surface current on the other patch. The radiation beams are tilted toward each other as the radiation pattern state I described in Fig. 3. Thus, the channel correlation will become worse for the MIMO system. Based on the analysis above, the two EBG structures are employed in the reference antenna to control the radiation beam for a better channel isolation. Meanwhile, for simplicity, the reference MIMO antenna, MIMO antenna with EBG1 and MIMO antenna with the two EBG structures are expressed as type I, type II and type III respectively. Considering the limited space for type I, one row of the EBG1 structures is first placed in the middle of the two patch elements. Thanks to the forbidden band characteristic, the surface wave between the two patch elements is suppressed. Thus, the coupling current on the

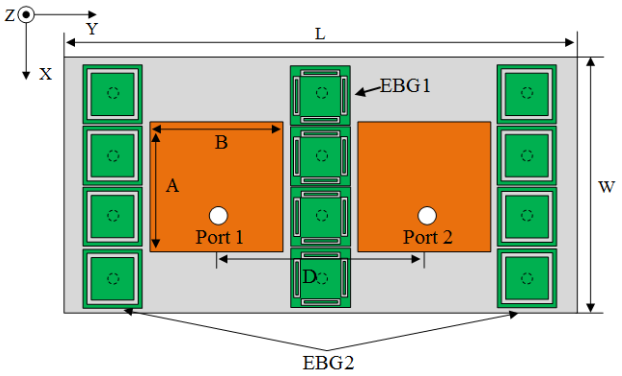

FIGURE 5. Front view of the MIMO antenna with EBG1 and EBG2.

TABLE 1. Parameters of the proposed antenna (unit: mm).

Parameters	Value	Parameters	Value
P_1	6.4	d_2	0.6
W_1	6.3	g_2	0.2
d_1	0.5	L	54
S_1	4.3	W	27
S_2	4.1	A	13.8
P_2	6.5	B	14
W_2	6.3	D	22

patch without excitation can be significantly reduced and the beam direction of one excited element is changed from state I to state II. Then the correlation coefficient as well as mutual coupling can be reduced preliminarily. To further improve ECC, two rows of EBG2 structures are placed on the outer edges of the two patches individually to support TM surface wave propagation. Therefore, the surface current can be guided to the EBG2 structures, which leads to radiation pattern state III. Meanwhile, to confirm this assumption, the surface current distributions of the three types at 4.95GHz are provided in Fig. 4. Moreover, because the two radiation beams are deflected to both edges individually, the space coupling wave is also decreased resulting in the higher port isolation. The structure of the MIMO antenna with the two EBG structures is shown in Fig. 5. The optimized parameters are described in table I.

Fig. 6 shows the simulated S-parameters of the three MIMO antennas. It can be seen that the working frequency band spanning from 4.82GHz to 5GHz (fractional bandwidth of about 3.7%) does not change for the three MIMO antennas. More importantly, compared with the S21 of type I, there is an evident mutual coupling reduction of 9dB for type III. The S21 is lower than −23dB within the operating bandwidth. The far field characteristic is also analyzed as follows to investigate the ECC.

When port 1 is excited and port 2 is matched with 50Ω load, the simulated radiation patterns of the three MIMO antennas are presented in Fig. 7. It is clearly observed that after the application of the two EBG structures, the beam direction can be tilted by −20°, relative to the normal direction.

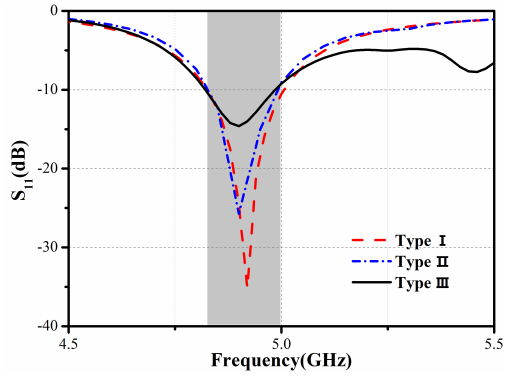

(a)

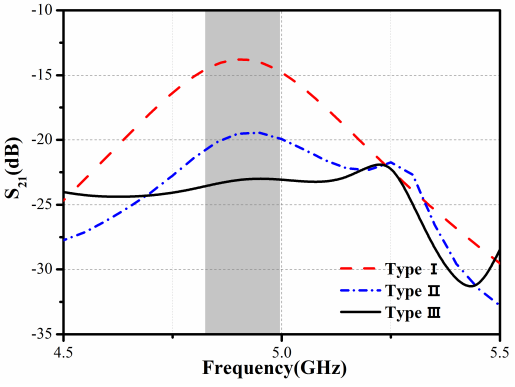

(b)

FIGURE 6. S-parameters of the three MIMO antennas. (a) S_{11}, (b) S_{21}.

The simulated corresponding maximum realized gain and radiation efficiency is provided in Fig. 7 (b). It is known that compared with the reference antenna, the gain of the MIMO antenna with the two EBG structures is decreased a little. Fig. 7 (c) shows the transformation of the 3D radiation pattern from state I to state III, which significantly avoids the interference between the two radiation beams so as to improve the channel isolation. The simulated ECC values of the three types are provided in Fig. 8. It is found that the ECC value of type III is lower than 4e-4 within the operating bandwidth and are much lower than that of type I.

C. DEFECTED GROUND STRUCTURE

Defected ground structure as a decoupling structure is commonly used as the stop band filter which can block the coupling surface current to flow from one antenna element to another in the frequency band of interest like in [15]–[18]. However, a new DGS is investigated based on the ground current of type III. It is found that the proposed DGS can control the polarization of the coupling field and a good mutual coupling reduction is obtained. DGS is made up of two "C" slots and a rectangular slot. Analyzing the port isolation of type III, it is known that mutual coupling is reduced by only 9dB, due to one row of arrangement of EBG1, which limits the capability of surface wave suppression. Therefore, to further

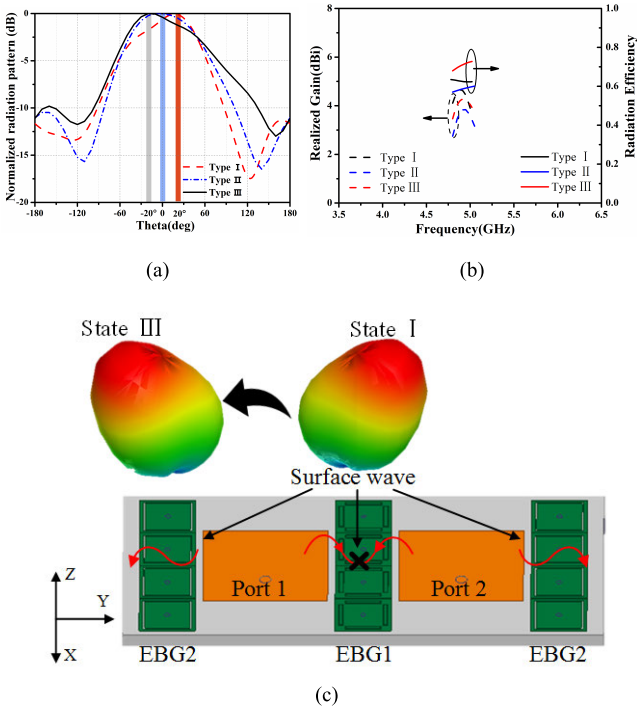

FIGURE 7. The radiation patterns of one patch antenna at 4.95GHz. (a) Normalized YOZ-plane radiation pattern of three states (b) simulated maximum antenna gain and radiation efficiency. (c) The 3D radiation patterns.

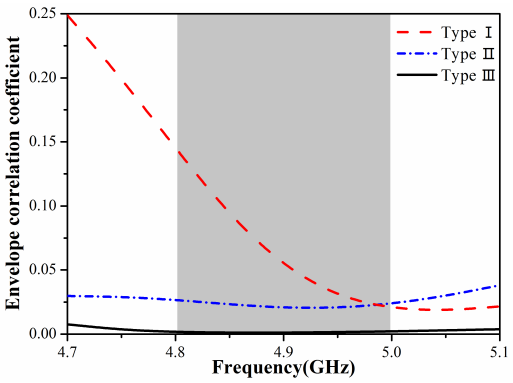

FIGURE 8. The simulated ECC of the MIMO antennas.

reduce the mutual coupling between the two patch antennas, the presented DGS is etched onto the ground of type III. Fig. 9 shows the back view of the structure named type IV. By adjusting the length and width of the slots, a better port isolation will be achieved. Fig. 10 shows that the S_{21} is influenced by different lengths of e_1. With increasing length e_1, the stop band shifts to the lower frequency band and mutual coupling reduction becomes weaker, yet the S_{11} remains unaltered. After optimization, the final structure parameters are provided as follows: $e_1 = 9.7$mm, $e_2 = 4.4$mm, $e_3 = 12$mm, $e_4 = 9$mm, $C_1 = 0.8$mm, $C_2 = 0.2$mm, and $C_3 = 0.2$mm.

To thoroughly figure out the working mechanism of the proposed DGS, the ground surface current is studied, which

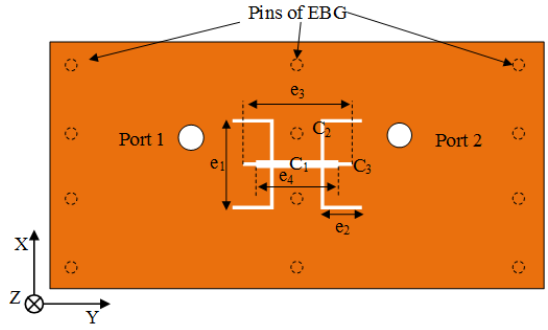

FIGURE 9. Back view of type IV.

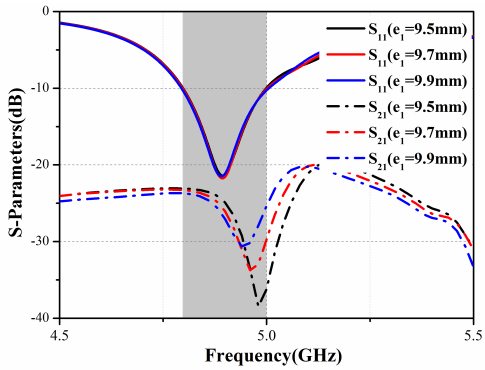

FIGURE 10. Parameter analysis of S_{21} with the length e_1 for type IV.

can be seen in Fig. 11. Compared with type I, the coupling current in the middle of the ground is disturbed for type III, because of the metallic via. However, the ground current distribution under the patch which is without excitation is barely influenced. Then, to control the coupling surface current direction, the proposed DGS is placed where the current direction is disordered, so as to guide the current to flow along the slot. Therefore, the ground surface current direction under the patch matched without 50Ω load is changed, as plotted in Fig. 11 (c). The coupling surface current distributions on the microstrip patches are provided in Fig. 12, which can be observed more distinctly. Contrasting type I and type III, the coupling surface current becomes weaker for type III, due to the hybrid EBG structures. Yet, the current direction is not altered. Furthermore, it can be seen from type IV that the coupling surface current direction is approximately changed from the X-direction to the Y-direction compared with type I, so that the polarization of the coupling field is perpendicular to that of the radiation element. Accordingly, the mutual coupling between the two patches can be reduced. Also because of no extra superstrate, the MIMO antenna can still maintain the low profile of 0.02λ.

Fig. 13 plots the S-parameters of type IV. It is found that the operating bandwidth spanning from 4.8GHz to 5GHz is wider than that of the reference MIMO antenna. Furthermore, DGS does not bring about the frequency shift like [16] and is mainly used to improve the port isolation that is described

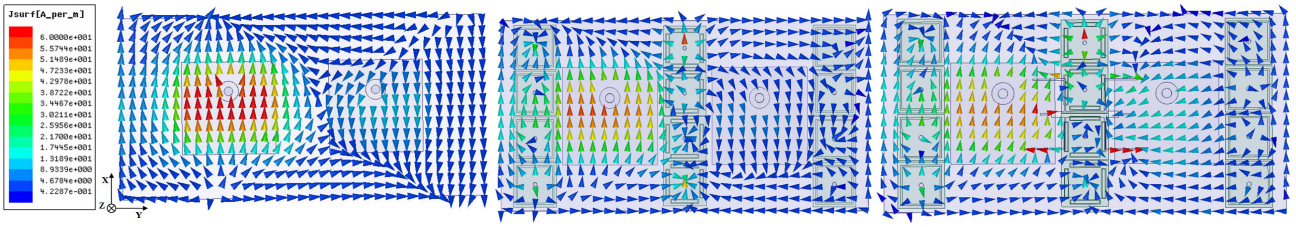

FIGURE 11. Ground Surface current distributions of type I type III and type IV at 4.95GHz.

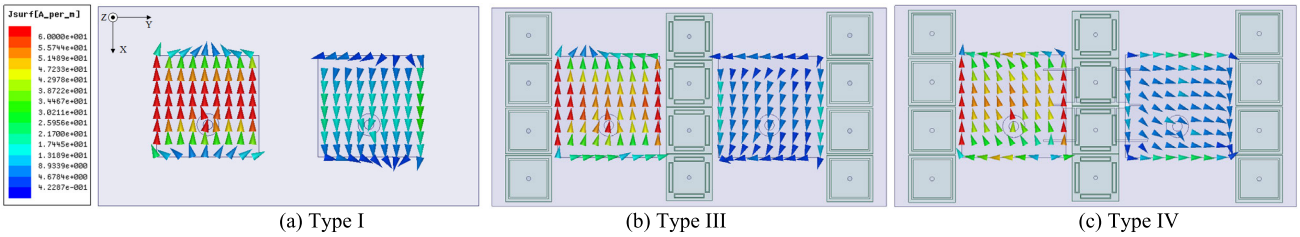

FIGURE 12. Surface current distributions on patches of type I, type III and type IV at 4.95GHz.

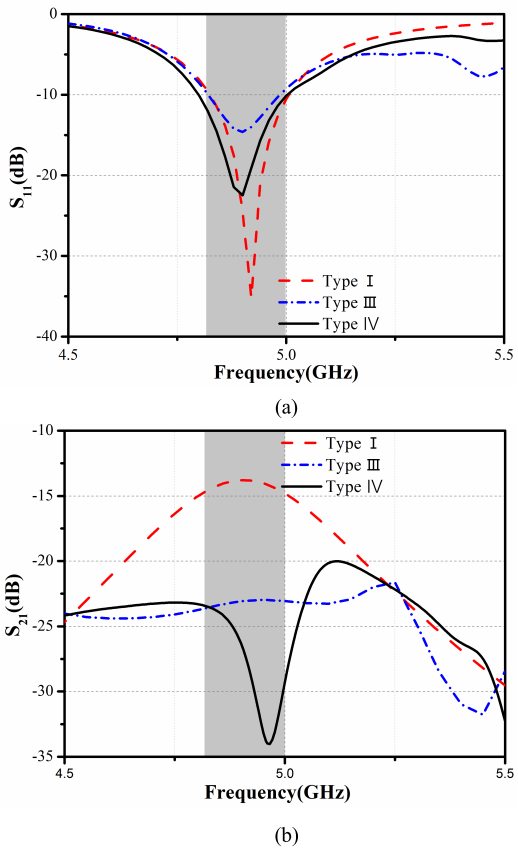

FIGURE 13. S-parameters of the proposed antenna. (a) S11, (b) S21.

in Fig. 13 (b). The maximum mutual coupling reduction of 20dB is obtained. The average isolation enhancement is about 14dB within the working frequency band.

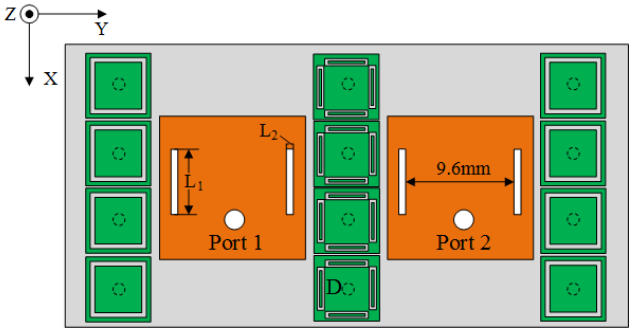

FIGURE 14. Front view of the proposed MIMO antenna.(L_1 = 4.2mm, L_2 = 0.3mm).

Moreover, it should be mentioned that the cross polarization of the antenna becomes worse, because of the orthogonal coupling current. Hence, to improve the cross polarization of the antenna, a pair of rectangular slots is etched on the patch along the current direction, which can avoid affecting the resonant frequency and the radiation characteristic of the antenna effectively. The structure of the proposed antenna is shown in Fig. 14. Compared with type IV, the cross polarization of the antenna seen in Fig.15 is improved. The cross polarization ratio of the proposed MIMO antenna is higher than 17dB in the maximum radiation direction. Also the cross polarization ratio is higher than 11dB within ±60°, which is acceptable for the MIMO antenna application. Fig.16 shows the S-parameters of the proposed antenna which has a good coincidence with that of type IV. Additionally, DGS and the rectangular slot have little impact on the maximum radiation beam direction, so that better ECC performance still can be maintained. Table II shows the simulated ECC value of the proposed antenna. Compared with type III and IV, although

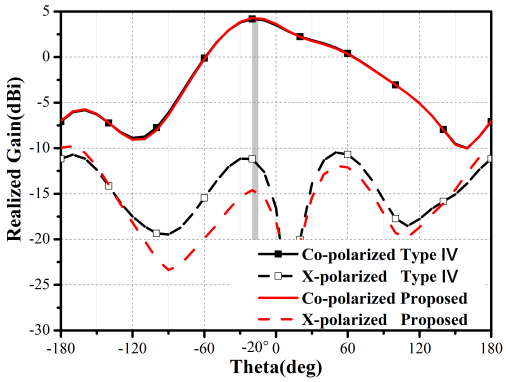

FIGURE 15. Simulated YOZ plane radiation patterns of the proposed MIMO antenna element at 4.95GHz.

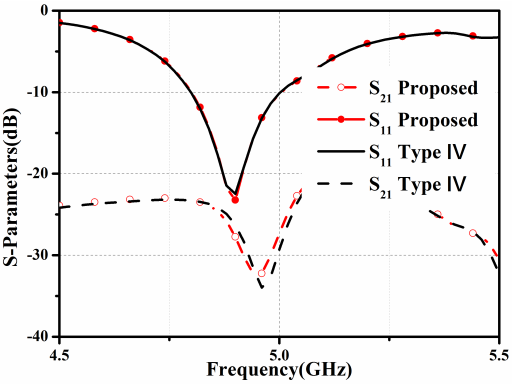

FIGURE 16. Simulated S-parameters of the proposed MIMO antenna.

TABLE 2. Envelope correlation coefficient of the proposed MIMO antenna.

ECC / Frequency	Type III	Type IV	Proposed antenna
4.78GHz	4.03e-4	0.05e-4	1.61e-4
4.82 GHz	1.91e-4	0.03e-4	1.47e-4
4.86 GHz	1.32e-4	0.29e-4	3.05e-4
4.9 GHz	1.31e-4	1.73e-4	5.4e-4
4.94 GHz	1.45e-4	2.51e-4	2.66e-4
4.98 GHz	1.42e-4	0.96e-4	0.57e-4
5.00 GHz	1.30e-4	0.56e-4	0.39e-4

the correlation coefficient of the proposed MIMO antenna is increased slightly around 4.9GHz, the ECC value is lower than 5.5e-4 within the working bandwidth.

III. RESULT AND DISCUSSION

To validate the proposed antenna design, the MIMO antenna is fabricated and measured. Fig. 17 shows the manufactured photos of the proposed MIMO antenna. The S-parameters are measured by an Agilent 8719ES vector network analyzer. The far field performances are measured in an anechoic chamber.

The measured S-parameters of the proposed MIMO antenna are plotted in Fig. 18. The measured −10dB

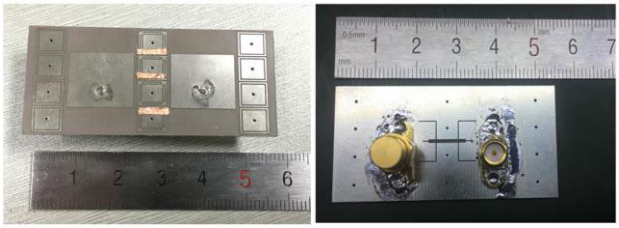

FIGURE 17. Fabricated photographs of the proposed MIMO antenna.

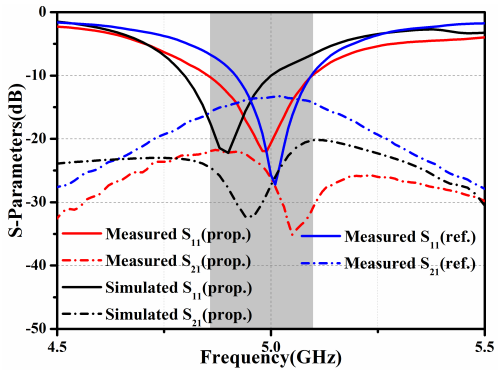

FIGURE 18. Measured S-parameters of the proposed MIMO antenna.

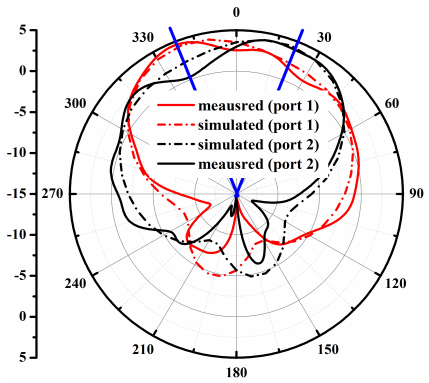

FIGURE 19. Measured H-plane total radiation patterns of the proposed MIMO antenna at 4.95GHz.

impedance bandwidth spans from 4.85GHz to 5.08GHz and the fractional bandwidth is about 4%. The minimum value of the measured S_{21} is about −35dB.

Fig. 19 shows the radiation pattern of the MIMO antenna at 4.95GHz in the H-plane. The measured beam direction is deflected by about 20°, which shows a good agreement with the simulated results. The deviation between simulated and measured results is mainly attributed to the manufactured errors. The measured mistake which cannot be excluded may be lead to the difference too.

The measured correlation coefficient is also provided in Fig. 20. It is known from [19], [22] that a low correlation coefficient of the proposed MIMO antenna indicates the good channel isolation is obtained. Thus the channel capacity can be improved a lot.

TABLE 3. Comparison between the previous works and the proposed MIMO antenna.

Ref.	Size(λ)	Center to center spacing(λ)	ECC	Maximum MC reduction(dB)	Technique		Antenna Type
					Diversity	Decoupling	
[3]	0.41×0.41×0.04 (four elements)	0.16	< 0.08	(S_{21}<-18.4)	Polarization and Radiation pattern	Metal strip and wall	Patch antenna
[4]	1.83×1.83×0.25 (two elements)	0.52	< 0.04	~8(S_{21}<-16)	Radiation pattern	FSS	Patch antenna
[5]	0.96×0.96×0.17 (four elements)	0.5	< 0.02	42(S_{21}<-42)	Polarization	EBG	Slot antenna
[6]	1.4×0.96×NA (two elements)	0.17	< 0.02	10(S_{21}<-27)	NA	Decoupling network	Monopole antenna
[11]	0.95×0.68×0.18 (two elements)	0.26	< 0.08	27(S_{21}<-41)	NA	Decoupling superstrate	Patch antenna
proposed	0.88×0.44×0.02 (two elements)	0.36	< 0.0006 (sim.) <0.002(mea.)	20(S_{21}<-33) (sim.) 22(S_{21}<-35)(mea.)	Radiation pattern	EBG+DGS	Patch antenna

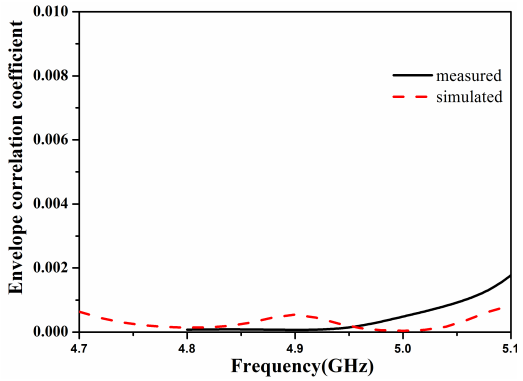

FIGURE 20. Calculated correlation coefficient of the proposed MIMO antenna.

Table III shows the comparison between the previous works and the proposed MIMO antenna. Designs discussed in [4], [5], [11] realize low ECC and high isolation (especially for [5], [11]), but the higher profile is an urgent problem needed to be addressed. For [3], the ECC of the antenna is relative high, although the radiation pattern and polarization diversity are utilized and the antenna has a relative compact size. More importantly, it is known that the proposed antenna design has very low correlation coefficients contrasting with the other works and the port isolation is also improved. In addition, the antenna structure has a very low profile.

IV. CONCLUSION

An extremely low correlation and high port isolation MIMO antenna based on hybrid EBG structures and DGS has been presented. To improve channel isolation, hybrid EBG structures that can control surface wave propagation were designed to realize the radiation pattern diversity. Meanwhile, as for the MIMO antenna with two EBG structures, a new defected ground structure was applied to the continuous ground. The proposed DGS could control the polarization of the coupling field. Therefore, a significant mutual coupling reduction was achieved. Then the rectangular slots were employed in the patch to decrease cross polarization. In addition, because of no extra superstrate used, a compact size of the MIMO antenna is realized, which makes the MIMO antenna a good candidate for 5G MIMO user terminals.

REFERENCES

[1] C. Rhee, Y. Kim, T. Park, S.-S. Kwoun, B. Mun, B. Lee, and C. Jung, "Pattern-reconfigurable MIMO antenna for high isolation and low correlation," *IEEE Antennas Wireless Propag. Lett.*, vol. 13, pp. 1373–1376, 2014.

[2] A. Ramachandran, S. V. Pushpakaran, M. Pezholil, and V. Kesavath, "A four-port MIMO antenna using concentric square-ring patches loaded with CSRR for high isolation," *IEEE Antennas Wireless Propag. Lett.*, vol. 15, pp. 1196–1199, 2016.

[3] A. Boukarkar, X. Q. Lin, Y. Jiang, L. Y. Nie, P. Mei, and Y. Yu, "A miniaturized extremely close-spaced four-element dual-band MIMO antenna system with polarization and pattern diversity," *IEEE Antennas Wireless Propag. Lett.*, vol. 17, no. 1, pp. 134–137, Jan. 2018.

[4] T. Hassan, M. U. Khan, H. Attia, and M. S. Sharawi, "An FSS based correlation reduction technique for MIMO antennas," *IEEE Trans. Antennas Propag.*, vol. 66, no. 9, pp. 4900–4905, Sep. 2018.

[5] G. Zhai, Z. N. Chen, and X. Qing, "Enhanced isolation of a closely spaced four-element MIMO antenna system using metamaterial mushroom," *IEEE Trans. Antennas Propag.*, vol. 63, no. 8, pp. 3362–3370, Aug. 2015.

[6] L. Zhao and K.-L. Wu, "A dual-band coupled resonator decoupling network for two coupled antennas," *IEEE Trans. Antennas Propag.*, vol. 63, no. 7, pp. 2843–2850, Jul. 2015.

[7] S. Zhang, Z. Ying, J. Xiong, and S. He, "Ultrawideband MIMO/diversity antennas with a tree-like structure to enhance wideband isolation," *IEEE Antennas Wireless Propag. Lett.*, vol. 8, pp. 1279–1282, 2009.

[8] S. Shoaib, I. Shoaib, N. Shoaib, X. Chen, and C. G. Parini, "Design and performance study of a dual-element multiband printed monopole antenna array for MIMO terminals," *IEEE Antennas Wireless Propag. Lett.*, vol. 13, pp. 329–332, 2014.

[9] A. Kaabal, M. El Halaoui, and A. Asselman, "A low mutual coupling design for array microstrip antennas integrated with electromagnetic bandgap structures," *Procedia Technol.*, vol. 22, pp. 549–555, 2016.

[10] S. Ghosh, T.-N. Tran, and T. Le-Ngoc, "Dual-layer EBG-based miniaturized multi-element antenna for MIMO systems," *IEEE Trans. Antennas Propag.*, vol. 62, no. 8, pp. 3985–3997, Aug. 2014.

[11] Z. Wang, L. Zhao, and Y. Cai, "A meta-surface antenna array decoupling (MAAD) method for mutual coupling reduction in a MIMO antenna system," *Sci. Rep.*, vol. 8, no. 1, 2018, Art. no. 3152.

[12] K.-L. Wu, C. Wei, X. Mei, and Z.-Y. Zhang, "Array-antenna decoupling surface," *IEEE Trans. Antennas Propag.*, vol. 65, no. 12, pp. 6728–6738, Dec. 2017.

[13] A. Jafargholi, A. Jafargholi, and H. Jun Choi, "Mutual coupling reduction in an array of patch antennas using CLL metamaterial superstrate for MIMO applications," *IEEE Trans. Antennas Propag.*, vol. 67, no. 1, pp. 179–189, Jan. 2019.

[14] M. Li, B. G. Zhong, and S. W. Cheung, "Isolation enhancement for MIMO patch antennas using near-field resonators as coupling-mode transducers," *IEEE Trans. Antennas Propag.*, vol. 67, no. 2, pp. 755–764, Feb. 2019.

[15] J. Ouyang, F. Yang, and Z. M. Wang, "Reducing mutual coupling of closely spaced microstrip MIMO antennas for WLAN application," *IEEE Antennas Wireless Propag. Lett.*, vol. 10, pp. 310–313, 2011.
[16] K. Wei, J.-Y. Li, L. Wang, Z.-J. Xing, and R. Xu, "Mutual coupling reduction by novel fractal defected ground structure bandgap filter," *IEEE Trans. Antennas Propag.*, vol. 64, no. 10, pp. 4328–4335, Oct. 2016.
[17] A. Habashi, J. Nourinia, and C. Ghobadi, "Mutual coupling reduction between very closely spaced patch antennas using low-profile folded split-ring resonators (FSRRs)," *IEEE Antennas Wireless Propag. Lett.*, vol. 10, pp. 862–865, 2011.
[18] L. Wang, Z. Xing, K. Wei, R. Xu, and J. Li, "S-shaped periodic defected ground structures to reduce microstrip antenna array mutual coupling," *Electron. Lett.*, vol. 52, no. 15, pp. 1288–1290, Jul. 2016.
[19] M. S. Sharawi, "Current misuses and future prospects for printed multiple-input, multiple-output antenna systems [wireless corner]," *IEEE Antennas Propag. Mag.*, vol. 59, no. 2, pp. 162–170, Apr. 2017.
[20] A. Aminian, F. Yang, and Y. Rahmat-Samii, "Bandwidth determination for soft and hard ground planes by spectral FDTD: A unified approach in visible and surface wave regions," *IEEE Trans. Antennas Propag.*, vol. 53, no. 1, pp. 18–28, Jan. 2005.
[21] R. G. Vaughan and J. B. Andersen, "Antenna diversity in mobile communications," *IEEE Trans. Veh. Technol.*, vol. 36, no. 4, pp. 149–172, Nov. 1987.
[22] J. X. Yun and R. G. Vaughan, "Multiple element antenna efficiency and its impact on diversity and capacity," *IEEE Trans. Antennas Propag.*, vol. 60, no. 2, pp. 529–539, Feb. 2012.

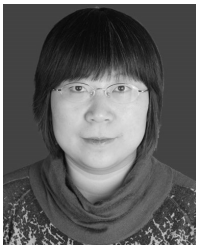

YING LIU (SM'17) received the B.Eng., M.S., and Ph.D. degrees in electromagnetics from Xidian University, Xi'an, China, in 1998, 2001, and 2004, respectively.

From 2006 to 2007, she carried on Postdoctoral Research in Hanyang University, Seoul, South Korea. She is currently a Full Professor with the National Key Laboratory of Science and Technology on Antennas and Microwaves, Xidian University. She is also a Full Professor and the Director of the National Key Laboratory of Science and Technology on Antennas and Microwaves. She has authored or coauthored over100 refereed journal articles. She has also authored *Prediction and Reduction of Antenna Radar Cross Section* (Xi'an: Xidian Univ. Press, 2010), and *Antennas for Mobile Communication Systems* (Beijing: Electronics Industry Press, 2011). Her research interests include antenna theory and technology, prediction, and control of antenna RCS. Prof. Liu is also a Senior Member of Chinese Institute of Electronics (CIE) and a Fellow of IET. She is also the Reviewer of several international journals and serves as a TPC member or Session Chair for several IEEE flagship conferences. She was a recipient of "New Century Excellent Talents in University" of the Ministry of Education for China, in 2011. She serves as an Associate Editor for IEEE Access.

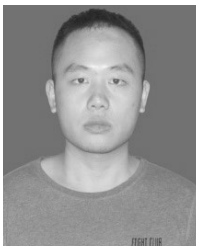

XU YANG was born in Ankang, Shaanxi, China, in 1992. He received the B.E. degree in electronic science and technology from the Xi'an University of Posts and Telecommunications, Xi'an, China, in 2014. He is currently pursuing the Ph.D. degree with Xidian University, Xi'an. His research interests include omnidirectional antennas, metasurfaces, and antenna array.

YONGTAO JIA was born in Tangshan, Hebei, China, in 1989. He received the B.Eng. and Ph.D. degrees in electromagnetics from Xidian University, Xi'an, China, in 2012 and 2017, respectively, where he is currently a Postdoctoral Fellow. His research interests include antenna RCS reduction, metasurface, and wideband phased arrays.

Y. JAY GUO received the B.S. and M.S. degrees from Xidian University, Xi'an, China, in 1982 and 1984, respectively, and the Ph.D. degree from Xian Jiaotong University, Xi'an, in 1987, all in electromagnetics.

Prior to this appointment in 2014, he served as a Research Director in CSIRO for over nine years, managing a number of ICT research portfolios. Before joining CSIRO, he held various senior leadership positions with Fujitsu, Siemens, and NEC, London, U.K. He is currently a Distinguished Professor and the Director of the Global Big Data Technologies Centre, University of Technology Sydney (UTS), Sydney, NSW, Australia. His research interests include reconfigurable antennas, conformal and wideband arrays, metamaterial, millimeter-wave and THz communications, and sensing systems. Dr. Guo is also a member of the College of Experts of Australian Research Council (ARC), and a Fellow of the Australian Academy of Engineering and Technology and IET. He was a recipient of a number of prestigious Australian national awards, and was named one of the most influential engineers in Australia, in 2014 and 2015. He has chaired numerous international conferences. He is the International Advisory Committee Chair of the IEEE VTC2017, a General Chair of ISAP2015, iWAT2014, and WPMC'2014, and a TPC Chair of 2010 IEEE WCNC, and 2012 and 2007 IEEE ISCIT. He serves as a Guest Editor for special issues on *Antennas for Satellite Communications* and *Antennas and Propagation Aspects of 60–90 GHz Wireless Communications,* both in the IEEE Transactions on Antennas and Propagation, and Special Issue on *Communications Challenges and Dynamics for Unmanned Autonomous Vehicles,* and the IEEE Journal on Selected Areas in Communications (JSAC).